

Anomalous Superfluid Density in a Disordered Charge-Density-Wave Material: Pd-Intercalated ErTe₃

Yusuke Iguchi^{1,2,3}, Joshua A. Straquadine^{2,3}, Chaitanya Murthy⁴, Steven A. Kivelson^{1,2,4},
Anisha G. Singh^{2,3}, Ian R. Fisher^{1,2,3} and Kathryn A. Moler^{1,2,3,4}

¹Stanford Institute for Materials and Energy Sciences, SLAC National Accelerator Laboratory,
2575 Sand Hill Road, Menlo Park, California 94025, USA

²Geballe Laboratory for Advanced Materials, Stanford University, Stanford, California 94305, USA

³Department of Applied Physics, Stanford University, Stanford, California 94305, USA

⁴Department of Physics, Stanford University, Stanford, California 94305, USA

 (Received 22 December 2023; revised 29 April 2024; accepted 21 May 2024; published 15 July 2024)

We image local superfluid density in single crystals of Pd-intercalated ErTe₃ below the superconducting critical temperature T_c , well below the onset temperature T_{CDW} of (disordered) charge-density-wave order. We find no detectable inhomogeneities on micron scales. We observe a rapid increase of the superfluid density below T_c , deviating from the behavior expected in a conventional Bardeen-Cooper-Schrieffer superconductor, and show that the temperature dependence is qualitatively consistent with a combination of quantum and thermal phase fluctuations.

DOI: [10.1103/PhysRevLett.133.036001](https://doi.org/10.1103/PhysRevLett.133.036001)

Pd_xErTe₃ is a model system for quasi-two-dimensional (2D) superconductivity and for the competition between charge-density-wave (CDW) and superconducting (SC) states. The superfluid density characterizes the phase stiffness of the superconducting order parameter and determines the London penetration depth $\lambda(T)$. In a conventional 3D Bardeen-Cooper-Schrieffer (BCS) superconductor, the temperature dependence of the normalized superfluid density $n_s(T) = \lambda^2(0)/\lambda^2(T)$ is controlled by the population of thermally excited Bogoliubov quasiparticles, and can be calculated using the Bogoliubov–de Gennes equations [1] or the semiclassical model [2]. At low temperatures, measurements of $n_s(T)$ provide information about the superconducting gap structure $\Delta(T, \mathbf{k})$. At temperatures close to T_c , however, the same theoretical considerations imply that $dn_s(T)/dT|_{T \rightarrow T_c}$ is not very sensitive to the gap structure, and changes somewhat but not dramatically in the strong-coupling and/or dirty limits [3,4].

$n_s(T)$ may have distinct features in quasi-2D conventional BCS superconductors. When the superconducting coherence length ξ is larger than the film thickness, the Berezinskii-Kosterlitz-Thouless (BKT) theory predicts an anomaly in the superfluid density at the BKT transition temperature [5–7]. More generally, strong phase fluctuations may suppress T_c and increase $dn_s(T)/dT|_{T \rightarrow T_c}$ [8]. Such anomalies have been observed in various ultrathin film superconductors, including Y_{1-x}Ca_xBa₂Cu₃O_{7- δ} [9], NbN [10], Pb [11], and *a*-MoGe [12].

We conducted measurements of the local diamagnetic susceptibility in Pd_xErTe₃ ($0 < x < 0.06$), a quasi-2D layered bulk superconductor, using scanning superconducting

quantum interference device (SQUID) microscopy (SSM) with micron-scale spatial resolution. Our results show that the superfluid density is homogeneous, with no detectable heterogeneity on micron scales. Additionally, we find non-BCS-like temperature dependence of the superfluid density with a steep slope $dn_s(T)/dT$ near T_c .

Recently, intertwined SC and CDW order has been observed in Pd-intercalated ErTe₃ [13–15]. The pristine “parent” compound ErTe₃ shows two, mutually transverse, in-plane, unidirectional, incommensurate CDW states [16], with no SC down to the measured lowest temperature, 100 mK [15]. Pd-intercalation induces disorder in the crystal lattice, suppressing CDW formation and leading to a SC ground state (Fig. 1) [14,15]. In crystals with a Pd concentration near $x = 0.05$, long-range CDW is not observed [17]. Scanning tunneling microscopy (STM) measurements of the tunneling conductance revealed a homogeneous SC gap at length scales exceeding the SC coherence length, and showed no direct correlation between the CDW and SC orders [15]. The anisotropic in-plane coherence lengths were estimated as $\xi_a \sim 1500$ Å and $\xi_c \sim 1000$ Å [15].

For this work, bulk single crystals of Pd-intercalated ErTe₃ were grown using the flux method [14]. We made images with a scanning SQUID susceptometer on cleaved *b* planes of Pd_xErTe₃ at temperatures varying from 0.3 to 3 K in a Bluefors LD dilution refrigerator for samples with $x = 0.003, 0.008, 0.018, 0.023, 0.029, 0.041, 0.054$. Our scanning SQUID susceptometer has a pickup loop that measures the local magnetic flux Φ in units of the flux quantum Φ_0 [18] while scanning with a pickup-loop-sample

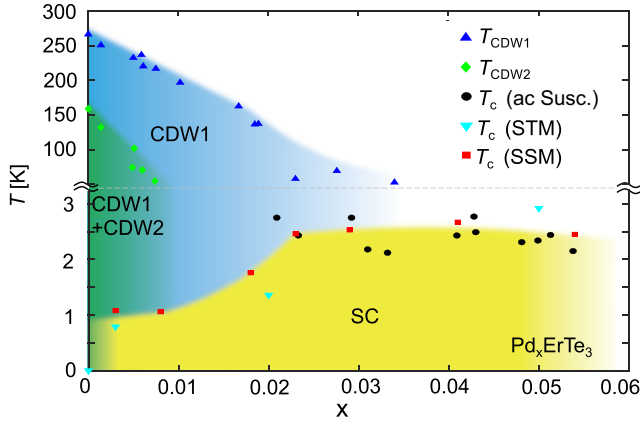


FIG. 1. Phase diagram of Pd-intercalated ErTe_3 . $T_{\text{CDW1,2}}$ from Ref. [14]. T_c determined by bulk ac susceptibility [14] and STM [15]. T_c obtained in this work (SSM) are plotted as red squares.

separation z , which we call the height. The minimum z can vary slightly between cooldowns and is 800 nm in these measurements (Supplemental Material [19]). The pickup loop is paired with a concentric field coil through which we apply an ac current of $|I^{\text{ac}}| = 1$ mA at a frequency of 1 kHz using an SR830 lock-in amplifier to produce a spatially varying localized ac magnetic field [18]. The maximum field applied to the sample surface with 1 mA currents is numerically estimated as 0.9 Oe in our configuration using SuperScreen [24], smaller than $H_{c1} \sim 2.5$ Oe at $0.89T_c$ in a sample with $x = 0.043$ [14]. We measure both quasistatic flux and the ac magnetic flux Φ^{ac} , and report the local ac susceptibility as $\chi = \Phi^{\text{ac}}/|I^{\text{ac}}|$ in units of Φ_0/A . Note that the imaginary part of χ did not have any height or location dependence in our measurements. SSM has been employed to image inhomogeneous superfluid responses in unconventional superconductors by detecting the local ac magnetic susceptibility [25–30]. By measuring the dependence of the local susceptibility on the scanning SQUID height, SSM enables estimation of the local London penetration depth λ [25,30–35].

To investigate the inhomogeneity of superfluid response, we imaged the local susceptibility at several temperatures. In all samples over the entire range of Pd concentrations explored, we observed sharp and apparently homogeneous transitions from the paramagnetic (PM) phase to the SC diamagnetic phase with T_c 's in the range $T_c = 0.8\text{--}2.8$ K [Fig. 2(a)]. The slight variation in the observed paramagnetic susceptibility above T_c among different Pd concentrations could represent the variation as a function of the doping but could also be due to differences in scan heights.

We analyze the susceptibility images by constructing a histogram of the number of pixels with a given amplitude of χ . The histograms show sharp peaks, indicating a relatively homogeneous sample. The spacing between pixels is

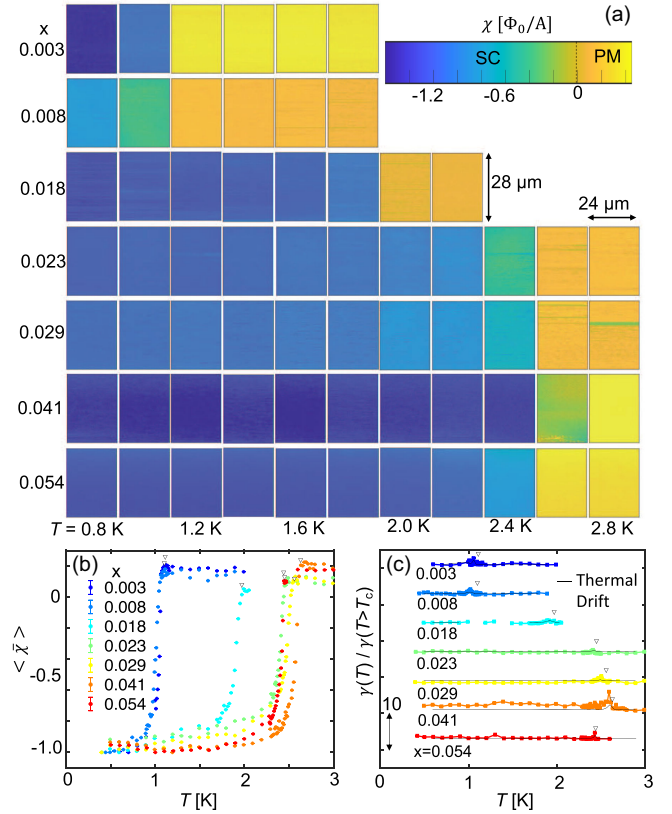


FIG. 2. Homogeneous superfluid density on micron scales in Pd_xErTe_3 . (a) Temperature dependence of local susceptibility images. (b) Normalized average susceptibilities show sharp drops just below T_c . (c) The standard deviation of the susceptibility shows only small peaks near T_c , consistent with thermal drift. Inverted triangles indicate T_c and solid lines are numerical calculations, including thermal drifting of ± 5 mK [19].

300 nm, and each pixel samples a micron-scale area determined by the geometry of the pickup loop and field coil. We choose a Gaussian function of the form $\mathcal{N} \exp[-(\chi - \beta)^2/2\gamma^2]$ to fit the peaks in the histogram (Supplemental Material Fig. S1 [19]). The normalized susceptibility averaged over the image is $\langle \bar{\chi} \rangle \equiv \beta(T)/\beta_{\text{min}}$, where β_{min} is the most negative value of $\beta(T)$. For certain doping levels, β_{min} does not equal β at the lowest temperatures, which can be attributed to noise. The upper limit on the inhomogeneity of the superfluid response on micron scales is characterized by the normalized standard deviation $\gamma(T)/\gamma(T > T_c)$. Plotting $\langle \bar{\chi} \rangle$ vs T , we see that T_c as a function of the Pd concentration [Fig. 2(b)] is consistent with previous measurements based on bulk susceptibility and STM measurements [14,15]. The apparent modest ratio of paramagnetic to diamagnetic susceptibility in our data aligns with previous findings [14]. This may stem from factors such as minimal susceptibility due to long penetration depths and pronounced paramagnetic susceptibility from the intrinsic magnetic properties of Er ions in Pd_xErTe_3 . More research is required to clarify

these effects, which are outside the scope of this study. The upper limits on the inhomogeneity exhibit small peaks just below T_c [Fig. 2(c)] and are consistent with a slight thermal drift during the scan (Supplemental Material Fig. S2 [19]). Thus, the superfluid response in Pd_xErTe_3 ($x = 0.003\text{--}0.054$) is consistent with homogeneity on a micron scale.

To determine the penetration depth, we measured susceptibility vs height [Fig. 3(a)]. The susceptibility is paramagnetic above T_c and diamagnetic below T_c . We fit the height dependence of the susceptibility [19] to a model that assumes a circular pickup loop of radius r' and field coil of radius r at a height z above the top of a film of thickness t on a substrate. The film is characterized by a London penetration depth λ and a paramagnetic permeability μ_2 . We

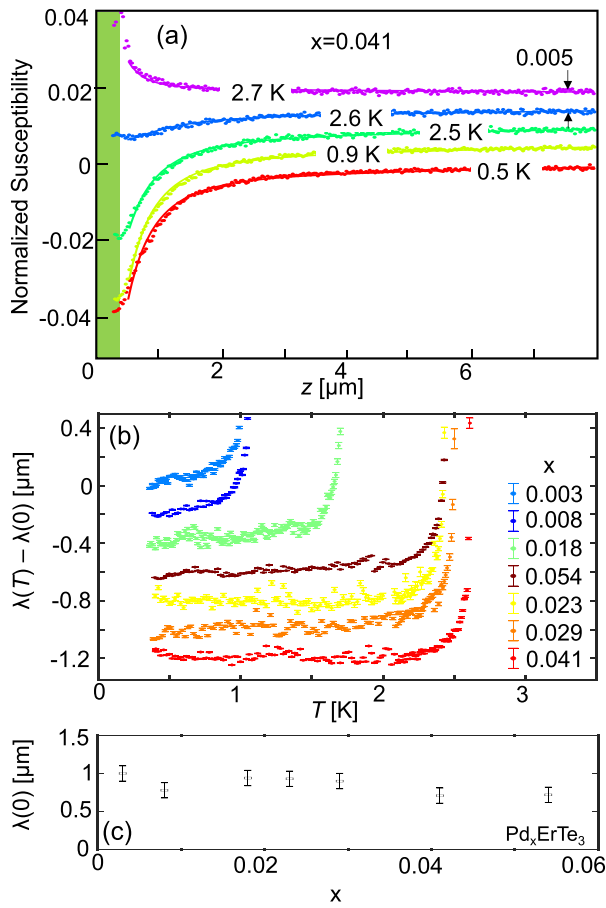


FIG. 3. Local susceptibility vs height provides $\lambda(T)$. (a) Height dependence of local normalized susceptibility in the $x = 0.041$ sample is well fitted by numerically calculated curves (solid lines) using Supplemental Material Eq. (S4) [19] with $\lambda(T)$ as a fitting parameter. The green-color-filled area indicates the distance between the pickup loop’s center and the sample surface when the SQUID tip touches the surface [19]. (b) Temperature dependence of the penetration depth obtained from the fitting results of Fig. 2(a) are plotted with an offset of 200 nm. (c) Estimated penetration depth at $T = 0$.

estimate the permeability $\mu_2 = 1.03\mu_0$, where μ_0 is the permeability of vacuum, by fitting the height dependence of the paramagnetic susceptibility above $T > T_c$ to Supplemental Material Eq. (S4) [19] with fixed parameters t , r' , r , and free parameter μ_2 . We then estimate $\lambda(T)$ by fitting susceptibility vs z for each value of $T < T_c$ to Supplemental Material Eq. (S4) [19] with fixed parameters t , r' , r , and μ_2 , a copper substrate permeability $\mu_3 = \mu_0$, and free parameter $\lambda(T)$.

The penetration depth does not depend strongly on the temperature at low temperatures [Fig. 3(b)]. We estimate $\lambda(T = 0)$ across the doping series to be in the range of 700–1000 nm, consistent with measurements of an isolated vortex field (Supplemental Material Fig. S3 [19]). This penetration depth is a factor of 3.5–5 larger than the only other estimate of λ in this material of which we are aware, which was an indirect estimate from the lower critical magnetic field at $T/T_c \sim 0.7$ for an $x = 0.043$ sample [15]. The error bars shown in the figure include all sources of errors of which we are aware (Supplemental Material [19]). Interestingly, we did not observe a significant dependence of $\lambda(T = 0)$ on the Pd-intercalation concentration [Fig. 3(c)], which indicates that the slight variation in susceptibility at 0.8 K between different concentrations of Pd [Fig. 2(a)] is due to differences in scan heights. In BCS theory, λ^2 would be expected to decrease in proportion to the mean free path [36], so the flat dependence of $\lambda(0)$ on x suggests either that BCS theory does not apply or that x is not the main determining factor for the mean free path.

Using the obtained values of λ , we calculate the normalized superfluid density $n_s(T) = \lambda^2(0)/\lambda^2(T)$. Our results reveal a rapid increase of n_s with decreasing temperature just below T_c and a slower increase at lower temperatures [Fig. 4(a)]. This temperature dependence clearly deviates from the expectations of the conventional weak coupling s -wave model (BCS model).

To investigate whether the anomalous temperature dependence of n_s can be simply attributed to details of the gap structure or strong-coupling effects, we consider an anisotropic s -wave model. In this model, the superconducting gap is described as $\Delta(T, \mathbf{k}) = \Delta_0(T) \times g(\mathbf{k})$, where $\Delta_0(T)$ represents the temperature dependence of the gap, and $g(\mathbf{k})$ its angular variation on the Fermi surface [37]. The temperature dependence is approximated by the typical mean-field form $\Delta_0(T) = \Delta_0(0) \tanh[\pi T_c \sqrt{\alpha(T_c/T - 1)}/\Delta_0(0)]$, where $\Delta_0(0)$ is the gap magnitude at $T = 0$ and α is a parameter. For a gap with anisotropic s -wave symmetry on a 2D cylindrical Fermi surface, $g(\phi) = \sqrt{1 - \varepsilon \sin^2 \phi}$, where $\phi = 0$ and $\pi/2$ correspond to the a and c axes, respectively, and $\varepsilon = 1 - [\Delta_c(0)/\Delta_a(0)]^2$ (assuming that $0 < \Delta_c \leq \Delta_a$). We note that our model does not determine which axis has a larger gap amplitude, as we take an angular average for the normalized superfluid density. The fitting parameters in this

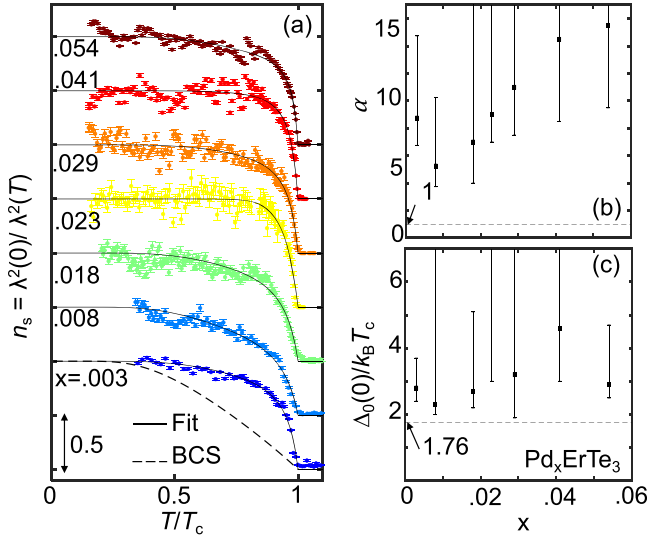


FIG. 4. Comparison of the estimated normalized superfluid density from Fig. 3(b) to an anisotropic s -wave BCS model. (a) Superfluid density (dots) and fits (solid lines) offset by 0.5. (b) Fitted values of α vs x . Values $\alpha \gg 1$ are physically unrealistic for known BCS models. (c) Fitted coupling constant $\Delta_0(0)/k_B T_c$ vs x .

model are $\Delta_0(0)$, ε , and α [19], and the normalized superfluid density is

$$n_i(T) = 1 - \frac{1}{2\pi T} \int_0^{2\pi} d\phi P_i(\phi) \times \int_0^\infty d\varepsilon \cosh^{-2} \left(\frac{\sqrt{\varepsilon^2 + \Delta^2(T, \phi)}}{2T} \right), \quad (1)$$

where $i = a, c$, and $P_a = \cos^2 \phi$, $P_c = \sin^2 \phi$. We find that our measured normalized superfluid density $n_s \simeq (n_a + n_c)/2$ can indeed be well fitted using Eq. (1) (for details of the fits, see the Supplemental Material [19]) (Fig. 4). However, the fitted parameter $\alpha \sim 10$ is much larger than known models, such as $\alpha = 1$ (isotropic s wave) and $\alpha = 2$ ($s + g$ wave) [37]. Such a large α induces an extraordinarily large $d\Delta(T)/dT|_{T \rightarrow T_c}$ (Supplemental Material Fig. S5 [19]). Moreover, the quality of the fit strongly depends on the value of α rather than the anisotropy ε or the coupling constant $\Delta_0(0)/k_B T_c$ (see Fig. S4 in Supplemental Material [19]). Thus, our fitting results suggest that the temperature-dependent superfluid density cannot fit the BCS model.

We next consider fluctuations, which can suppress T_c and modify the temperature dependence of the superfluid density. Quasi-2D electronic structures can enhance fluctuations [15,16]. A pure BKT scenario cannot be applied here, as the sample thicknesses exceed the coherence length. Classical phase fluctuations alone would destroy the SC order above $T_\theta = 7\text{--}14$ K estimated from formulas in Ref. [8] using $\xi = 100\text{--}150$ nm and $\lambda = 700\text{--}1000$ nm. Notably, this estimated T_θ is close to T_c , suggesting that

such phase fluctuations might significantly contribute to the determination of T_c . (Note that Fang *et al.* estimated T_θ as 170 K, much larger than T_c , from $\lambda = 200$ nm [15].) However, superfluid density that is dominated by classical phase fluctuations would exhibit a linear- T dependence well below T_c [38], not flattening until quantum effects become important. Therefore, classical phase fluctuations alone cannot explain our results.

Quantum phase fluctuations may modify this scenario. The small value of T_θ and the quasi-2D character of the electronic structure likely enhance the effectiveness of these fluctuations, which may be further enhanced [39] by a degree of randomness of the interlayer Josephson coupling produced by the Pd intercalation. To determine whether a combination of quantum and classical phase fluctuations might account for the observed anomalous T dependence of the superfluid density, we have studied a caricature of the problem in terms of the quantum rotor model on a 2D square lattice governed by the Hamiltonian

$$H = \sum_j \frac{n_j^2}{2C} - J \sum_{\langle i,j \rangle} \cos(\theta_i - \theta_j), \quad (2)$$

where n_j is the number of Cooper pairs on site j of the 2D lattice and satisfies the commutation relations $[n_i, n_j] = [e^{i\theta_i}, e^{i\theta_j}] = 0$ and $[n_i, e^{i\theta_j}] = \delta_{ij} e^{i\theta_j}$, C is a local capacitance which plays the role of an effective mass, and J is a measure of the phase stiffness within a plane. In this model, it is required that the mean-field critical temperature T_{MF} be considerably higher than T_c to assume local pairing over a broader range of T . (This model omits many possibly significant effects, including long-range Coulomb interactions and dissipation stemming from the existence of quasiparticle excitations.) For this model, we estimate the T -dependent superfluid density using the variational method used in [40] (for details, see the Supplemental Material [19]). The results for a range of coupling constants C and J capture some of the salient features of our experimental findings, as shown in Fig. 5(b), suggesting that strong quantum phase fluctuations are probably significant.

Finally, it is worth noting that T_c displays a complex variation with x as shown in Fig. 1, where T_c initially rises rapidly with x before approximately ‘‘saturating.’’ The fact that T_c does not decrease with the disorder at $x > 0.02$ might be attributed to Anderson’s theorem, but this theorem does not explain the initial rise relative to zero Pd concentration [41]. The x dependence of T_c likely reflects the complex interplay of a variety of factors, including the competition between CDW formation and superconductivity, the effects of disorder on the CDW state, and also the influence of quantum phase fluctuations on the superconducting state.

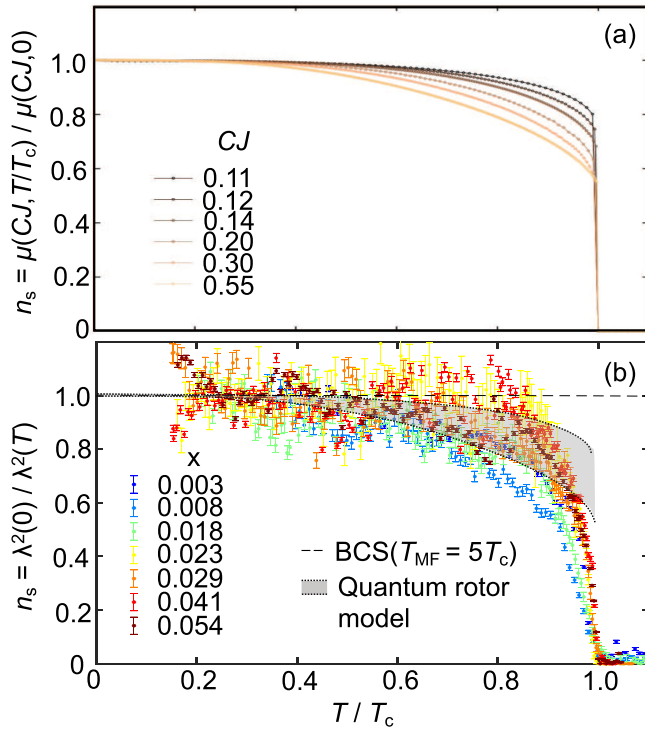


FIG. 5. Normalized superfluid density in the quantum rotor model compared to experimental results in Pd_xErTe_3 . (a) Variational solution of the quantum rotor model for several values of the coupling constant CJ . (b) The experimental results from Fig. 4(a) compared with the results of the quantum rotor model from Fig. 5(a) and Supplemental Material Fig. S5 [19]. For concreteness, we assume $T_{\text{MF}} = 5T_c$ in the BCS model.

In summary, we use scanning SQUID susceptometry to examine, at the microscopic level, the superfluid response on cleaved surfaces of Pd-intercalated ErTe_3 . Our findings reveal that the superfluid response is uniform on a micron scale within the Pd-intercalation-induced superconducting state, consistent with previous STM measurements. We also observe an unexpectedly strong (relative to BCS) temperature dependence of the superfluid density near T_c for all Pd concentrations. To explain this non-BCS-like temperature-dependent superfluid density in Pd_xErTe_3 , we employ the quantum rotor model. Our results suggest that quantum phase fluctuations suppress T_c and determine the functional form of $\lambda(T)$ in Pd_xErTe_3 . Moreover, our study highlights the potential of temperature-dependent superfluid density as a valuable tool for investigating quantum phase fluctuations in quasi-2D superconductors.

We thank A. Kapitulnik, A. Fang, and J. R. Kirtley for fruitful discussions. We also extend our gratitude to L. Bishop-Van Horn for his invaluable assistance with the simulations of applied magnetic fields. This work was primarily supported by the Department of Energy, Office of Science, Basic Energy Sciences, Materials Sciences and

Engineering Division, under Contract No. DE-AC02-76SF00515. Y.I. was partially supported by a JSPS Overseas Research Fellowship. C.M. was supported in part by the Gordon and Betty Moore Foundation's EPIQS Initiative through Grant No. GBMF8686.

- [1] T. Kita, *Statistical Mechanics of Superconductivity* (Springer, Tokyo, 2015).
- [2] B. S. Chandrasekhar and D. Einzel, *Ann. Phys. (N.Y.)* **2**, 535 (1993).
- [3] D. Xu, S. K. Yip, and J. A. Sauls, *Phys. Rev. B* **51**, 16233 (1995).
- [4] A. Maisuradze, R. Gumeniuk, W. Schnelle, M. Nicklas, C. Baines, R. Khasanov, A. Amato, and A. Leithe-Jasper, *Phys. Rev. B* **86**, 174513 (2012).
- [5] L. Benfatto, C. Castellani, and T. Giamarchi, *Phys. Rev. B* **77**, 100506(R) (2008).
- [6] V. L. Berezinskii, *Sov. Phys. JETP* **34**, 610 (1972), <https://inspirehep.net/literature/1716846>.
- [7] J. M. Kosterlitz and D. J. Thouless, *J. Phys. C* **5**, L124 (1972).
- [8] V. J. Emery and S. A. Kivelson, *Nature (London)* **374**, 434 (1995).
- [9] I. Hetel, T. R. Lemberger, and R. Mohit, *Nat. Phys.* **3**, 700 (2007).
- [10] A. Kamlapure, M. Mondal, M. Chand, A. Mishra, J. Jesudasan, V. Bagwe, L. Benfatto, V. Tripathi, and P. Raychaudhuri, *Appl. Phys. Lett.* **96**, 072509 (2010).
- [11] H. Nam, H. Chen, T. Liu, J. Kim, C. Zhang, J. Yong, T. R. Lemberger, P. A. Kratz, J. R. Kirtley, K. A. Moler, P. W. Adams, A. H. MacDonald, and C.-K. Shih, *Proc. Natl. Acad. Sci. U.S.A.* **113**, 10513 (2016).
- [12] S. Mandal, S. Dutta, S. Basistha, I. Roy, J. Jesudasan, V. Bagwe, L. Benfatto, A. Thamizhavel, and P. Raychaudhuri, *Phys. Rev. B* **102**, 060501(R) (2020).
- [13] J. B. He, P. P. Wang, H. X. Yang, Y. J. Long, L. X. Zhao, C. Ma, M. Yang, D. M. Wang, X. C. Shangguan, M. Q. Xue, P. Zhang, Z. A. Ren, J. Q. Li, W. M. Liu, and G. F. Chen, *Supercond. Sci. Technol.* **29**, 065018 (2016).
- [14] J. A. W. Straquadine, F. Weber, S. Rosenkranz, A. H. Said, and I. R. Fisher, *Phys. Rev. B* **99**, 235138 (2019).
- [15] A. Fang, A. G. Singh, J. A. W. Straquadine, I. R. Fisher, S. A. Kivelson, and A. Kapitulnik, *Phys. Rev. Res.* **2**, 043221 (2020).
- [16] N. Ru, C. L. Condon, G. Y. Margulis, K. Y. Shin, J. Laverock, S. B. Dugdale, M. F. Toney, and I. R. Fisher, *Phys. Rev. B* **77**, 035114 (2008).
- [17] A. Fang, J. A. W. Straquadine, I. R. Fisher, S. A. Kivelson, and A. Kapitulnik, *Phys. Rev. B* **100**, 235446 (2019).
- [18] J. R. Kirtley, L. Paulius, A. J. Rosenberg, J. C. Palmstrom, C. M. Holland, E. M. Spanton, D. Schiessl, C. L. Jernain, J. Gibbons, Y.-K.-K. Fung, M. E. Huber, D. C. Ralph, M. B. Ketchen, G. W. Gibson, Jr., and K. A. Moler, *Rev. Sci. Instrum.* **87**, 093702 (2016).
- [19] See Supplemental Material at <http://link.aps.org/supplemental/10.1103/PhysRevLett.133.036001> for (Sec. 1) the details of the calculations of inhomogeneity of superfluid response, (Sec. 2) the details of the isolated vortex

- field measurements, (Sec. 3) the estimate of the London penetration depth from the susceptibility measurements, (Sec. 4) the details of fitting the temperature-dependent superfluid density, (Sec. 5) and the detailed calculations of superfluid density in the quantum rotor model, which includes Refs. [20–23].
- [20] J. R. Kirtley, L. Paulius, A. J. Rosenberg, J. C. Palmstrom, D. Schiessl, C. L. Jermain, J. Gibbons, C. M. Holland, Y.-K.-K. Fung, M. E. Huber, M. B. Ketchen, D. C. Ralph, G. W. Gibson, Jr., and K. A. Moler, *Supercond. Sci. Technol.* **29**, 124001 (2016).
- [21] V. G. Kogan, *Phys. Rev. B* **68**, 104511 (2003).
- [22] F. Gross, B. S. Chandrasekhar, D. Einzel, K. Andres, P. J. Hirschfeld, H. R. Ott, J. Beuers, Z. Fisk, and J. L. Smith, *Z. Phys. B* **64**, 175 (1986).
- [23] S. Chakravarty, G.-L. Ingold, S. Kivelson, and A. Luther, *Phys. Rev. Lett.* **56**, 2303 (1986).
- [24] L. Bishop-Van Horn and K. A. Moler, *Comput. Phys. Commun.* **280**, 108464 (2022).
- [25] C. W. Hicks, T. M. Lippman, M. E. Huber, J. G. Analytis, J.-H. Chu, A. S. Erickson, I. R. Fisher, and K. A. Moler, *Phys. Rev. Lett.* **103**, 127003 (2009).
- [26] B. Kalisky, J. R. Kirtley, J. G. Analytis, J.-H. Chu, A. Vailionis, I. R. Fisher, and K. A. Moler, *Phys. Rev. B* **81**, 184513 (2010).
- [27] C. A. Watson, A. S. Gibbs, A. P. Mackenzie, C. W. Hicks, and K. A. Moler, *Phys. Rev. B* **98**, 094521 (2018).
- [28] I. P. Zhang, J. C. Palmstrom, H. Noad, L. Bishop-Van Horn, Y. Iguchi, Z. Cui, E. Mueller, J. R. Kirtley, I. R. Fisher, and K. A. Moler, *Phys. Rev. B* **100**, 024514 (2019).
- [29] L. B.-V. Horn, Z. Cui, J. R. Kirtley, and K. A. Moler, *Rev. Sci. Instrum.* **90**, 063705 (2019).
- [30] Y. Iguchi, H. Man, S. M. Thomas, F. Ronning, P. F. S. Rosa, and K. A. Moler, *Phys. Rev. Lett.* **130**, 196003 (2023).
- [31] L. Luan, T. M. Lippman, C. W. Hicks, J. A. Bert, O. M. Auslaender, J.-H. Chu, J. G. Analytis, I. R. Fisher, and K. A. Moler, *Phys. Rev. Lett.* **106**, 067001 (2011).
- [32] J. R. Kirtley, B. Kalisky, J. A. Bert, C. Bell, M. Kim, Y. Hikita, H. Y. Hwang, J. H. Ngai, Y. Segal, F. J. Walker, C. H. Ahn, and K. A. Moler, *Phys. Rev. B* **85**, 224518 (2012).
- [33] T. M. Lippman, B. Kalisky, H. Kim, M. A. Tanatar, S. L. Bud'ko, P. C. Canfield, R. Prozorov, and K. A. Moler, *Physica (Amsterdam)* **483C**, 91 (2012).
- [34] J. A. Bert, K. C. Nowack, B. Kalisky, H. Noad, J. R. Kirtley, C. Bell, H. K. Sato, M. Hosoda, Y. Hikita, H. Y. Hwang, and K. A. Moler, *Phys. Rev. B* **86**, 060503(R) (2012).
- [35] Y. Iguchi, I. P. Zhang, E. D. Bauer, F. Ronning, J. R. Kirtley, and K. A. Moler, *Phys. Rev. B* **103**, L220503 (2021).
- [36] M. Tinkham, *Introduction to Superconductivity*, 2nd ed. (Dover Publications, New York, 2004).
- [37] R. Prozorov and R. W. Giannetta, *Supercond. Sci. Technol.* **19**, R41 (2006).
- [38] E. W. Carlson, S. A. Kivelson, V. J. Emery, and E. Manousakis, *Phys. Rev. Lett.* **83**, 612 (1999).
- [39] E. Nakhmedov, O. Alekperov, and R. Oppermann, *Phys. Rev. B* **86**, 214513 (2012).
- [40] S. Chakravarty, G.-L. Ingold, S. Kivelson, and A. Luther, *Phys. Rev. Lett.* **56**, 2303 (1986).
- [41] P. W. Anderson, *J. Phys. Chem. Solids* **11**, 26 (1959).